

Revisiting the Flocking Transition Using Active Spins

A. P. Solon and J. Tailleur

Université Paris Diderot, Sorbonne Paris Cité, MSC, UMR 7057 CNRS, F75205 Paris, France

(Received 16 March 2013; published 13 August 2013)

We consider an active Ising model in which spins both diffuse and align on lattice in one and two dimensions. The diffusion is biased so that plus or minus spins hop preferably to the left or to the right, which generates a flocking transition at low temperature and high density. We construct a coarse-grained description of the model that predicts this transition to be a first-order liquid-gas transition in the temperature-density ensemble, with a critical density sent to infinity. In this first-order phase transition, the magnetization is proportional to the liquid fraction and thus varies continuously throughout the phase diagram. Using microscopic simulations, we show that this theoretical prediction holds in 2D whereas the fluctuations alter the transition in 1D, preventing, for instance, any spontaneous symmetry breaking.

DOI: [10.1103/PhysRevLett.111.078101](https://doi.org/10.1103/PhysRevLett.111.078101)

PACS numbers: 87.18.Gh, 05.65.+b, 45.70.Vn

Active matter systems are driven out of equilibrium by the injection of energy at the single particle level [1–4]. This microscopic breakdown of detailed balance results in a wide range of phenomena that have aroused the interest of physicists, from bacterial ratchets [5–8] to self-propelled clusters [9–11]. Furthermore, this rich phenomenology is often captured by simple models. For instance, simple flocking models account for the patterns found in motility assays [12,13] while bacterial clustering was successfully modeled using self-propelled rods [14].

Nevertheless, despite the successful description of many experiments, a full understanding of the underlying mechanisms sometimes remains elusive. For instance, even though the flocking transition is a central feature of active matter, it remains one of the most debated questions in the field. In their seminal work, Vicsek and co-workers [15] showed that self-propelled particles that align locally can exhibit a transition to long-range order in 2D. Initially thought to be continuous [15], this transition was later shown to be first order using large scale simulations and a finite size scaling akin to that of magnetic phase transitions [16]. Many works were also devoted to nematic [17–19] or metric-free interactions [20], the latter yielding a continuous transition [21]. Flocking models were also studied in 1D [22,23] where, surprisingly, the transition was found to be critical.

Obtaining conclusive numerical evidence for flocking models is notoriously difficult due to strong finite-size effects and the lack of a theoretical framework to analyze them. In parallel to numerical studies, much effort was thus devoted to construct such an analytical description of the flocking transition. While the Vicsek model (VM) is among the simplest to simulate, it is one of the hardest to coarse grain, being defined off lattice, in discrete time and involving manybody interactions. Many approaches were thus either phenomenological [24–26] or focused on simpler models [27], and progress is slower for the VM [28]. Lots of effort was also devoted to the nematic case [29–31] or to topologic interactions [30,32]. The existence of long-range

order in 2D for polar alignment was established [24] but progress is difficult since the coarse-grained equations are hard to solve. Most analytical studies were thus restricted to the linear stability analysis of homogeneous solutions or the simulation of continuous equations [25–27]. While non-linear profiles for a model with nematic alignment could be computed explicitly [30], closed analytical solutions are still missing for polar models despite recent progress [25,27,28]. All in all, despite the important progresses made during the last few years, a unifying theoretical framework of the flocking transition is still missing.

We present below a tentative step in this direction through the introduction of a microscopic lattice model with discrete symmetry, which is much simpler to study numerically and analytically than traditional flocking models. By bridging micro and macro, we show the transition of our model to amount to a standard liquid-gas transition in the canonical ensemble with an infinite critical density. This sheds new light on the finite-size scaling of the transition and predicts the order parameter to vary *continuously* in the temperature-density plane, in the thermodynamic limit. Furthermore, we show that there is no critical transition in 1D, where fluctuations strongly alter the transition.

We consider N particles carrying Ising spins $s = \pm 1$ on a 1D lattice of L sites. Each particle hops at rate $D(1 + s\varepsilon)$ and $D(1 - s\varepsilon)$ to its right and left neighboring site. (In higher dimensions, the hopping rates are symmetric in all but one directions.) There is no exclusion between particles and we note n_i^\pm the numbers of \pm spins on site i so that the local densities and magnetizations are given by $\rho_i = n_i^+ + n_i^-$ and $m_i = n_i^+ - n_i^-$. The particles also align their spins: on site i each spin s flips at rate $\exp(-sm_i/T\rho_i)$ where the temperature T plays a role similar to the orientational noise in the VM [16]. When $D = 0$, the system thus amounts to L^d independent fully connected Ising models. When $D > 0$ and $\varepsilon \neq 0$, three different configurations are typically observed (see Fig. 1): at low temperature a uniform ordered phase, at high temperature a uniform disordered phase,

and phase-separated profiles in between, with narrow interfaces connecting ordered high density bands ($\rho_i \approx \rho_h$, $m_i \approx m_h \neq 0$) to disordered homogeneous backgrounds ($\rho_i \approx \rho_\ell$, $m_i \approx 0$). These profiles are all long-lived in finite systems even though their stability in the thermodynamic limit depends on the number of spatial dimensions. Let us now show how a simple theoretical framework can be constructed to account for the phase diagram of Fig. 1.

Previous coarse-graining approaches often relied on factorization approximation of kinetic equations [27,29,33,34]. On a 1D lattice, this amounts to a mean-field approximation: $f(\langle n_i^\pm \rangle) = \langle f(n_i^\pm) \rangle$, which may be quantitatively wrong but often captures phase diagrams exactly [35,36]. Introducing $x = i/L$, $v = 2D\epsilon/L$, $\tilde{D} = D/L^2$, and $\beta = T^{-1}$, the mean-field dynamics of the coarse-grained fields $\rho(x) = \langle \rho_i \rangle$ and $m(x) = \langle m_i \rangle$ is given, in the large L limit, by

$$\dot{\rho} = \tilde{D} \partial_{xx} \rho - v \partial_x m \quad (1)$$

$$\dot{m} = \tilde{D} \partial_{xx} m - v \partial_x \rho + 2\rho \sinh \frac{\beta m}{\rho} - 2m \cosh \frac{\beta m}{\rho}. \quad (2)$$

In higher dimensions ∂_{xx} becomes a Laplacian Δ , and we use this more general form hereafter.

Looking for the onset of a flocking transition, we linearize the dynamics for $m \ll \rho$, which yields [37]

$$\dot{m} = \tilde{D} \Delta m - v \partial_x \rho + 2m(\beta - 1) - \alpha \frac{m^3}{\rho^2} \quad (3)$$

where $\alpha = \beta^2[1 - (\beta/3)]$. The line $\beta = 1$ separates the linear stability regions of homogeneous ordered and disordered profiles while simulations of Eqs. (1) and (2) never show stable phase-separated profiles [38]. The mean-field

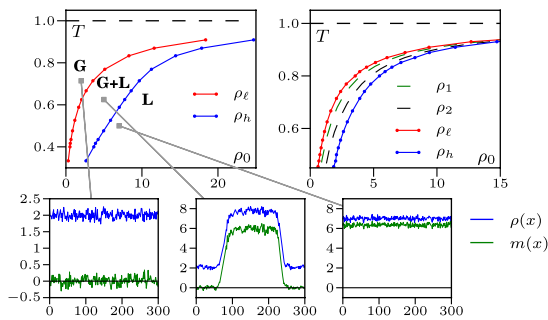


FIG. 1 (color online). Top left: Phase diagram in 2D with ordered liquid (L), disordered gas (G), and coexistence region ($G + L$). The red and blue lines correspond to low and high densities of phase separated profiles; they enclose the region where such profiles can be seen. $D = 1$, $\epsilon = 0.9$, $L = 300$, $\rho_0 = N/L$. Bottom: Snapshots of the different profiles averaged over the transverse direction. Top right: Phase diagram predicted by the RMFM. In addition to ρ_h and ρ_ℓ , black and green dashed spinodal lines signal the loss of linear stability of the homogeneous profiles. $D = v = r = 1$.

approximation thus predicts a continuous transition from $m \equiv (1/L) \sum_i m_i = 0$ to $m = m_0(\beta)$ at $\beta_c = 1$, in contradiction with Fig. 1. As often [39,40], the mean-field approximation is only valid for $\rho \rightarrow \infty$; for finite densities we thus expand the mean-field critical temperature to include $1/\rho$ corrections [41,42] and use $\beta_c \equiv 1 + (r/\rho)$ in Eq. (3):

$$\dot{m} = \tilde{D} \Delta m - v \partial_x \rho + 2m \left(\beta - 1 - \frac{r}{\rho} \right) - \alpha \frac{m^3}{\rho^2}. \quad (4)$$

The phase diagram corresponding to Eqs. (1) and (4), which form our refined mean-field model (RMFM), is presented in the top-right corner of Fig. 1. When $T < 1$, homogeneous disordered (resp. ordered) profiles are always linearly stable at low enough density $\rho_0 < \rho_1$ (resp. high enough density $\rho_0 > \rho_2$). Since $\rho_1 < \rho_2$, there is a finite intermediate region $[\rho_1, \rho_2]$ where neither homogeneous profiles are stable. In this region, the system separates into two homogeneous phases connected with sharp fronts: a disordered region with low density $\rho_\ell < \rho_1$ and an ordered region with high density $\rho_h > \rho_2$ and $m_h \neq 0$.

Propagating shocks can be computed analytically when β is close to 1 by linearizing Eq. (4) around the density $\rho_1 = r/(\beta - 1)$ at which the homogeneous disordered profile becomes linearly unstable. We first solve Eq. (1), by neglecting the diffusion term in a reference frame moving at speed c , to get ρ as a function of m :

$$\rho(\mathbf{r}) = \rho_\ell + \frac{v}{c} m(\mathbf{r}). \quad (5)$$

Equations (4) and (5) then yields for m

$$\tilde{D} \Delta m + c \left(1 - \frac{v^2}{c^2} \right) \partial_x m + \mu \left[\rho_\ell - \rho_1 + \frac{v}{c} m \right] m - \alpha \frac{m^3}{\rho_1^2} = 0 \quad (6)$$

where $\mu = 2r/\rho_1^2$. Looking for ascending ($q^+ > 0$) and descending ($q^- < 0$) front solutions

$$m(\mathbf{r}) = \frac{m_h}{2} [1 + \tanh(q^\pm x)] \quad (7)$$

one gets

$$c = v; \quad q^\pm = \frac{\pm m_h \sqrt{\alpha}}{\sqrt{8\tilde{D}\rho_1}}; \quad m_h = \frac{4r}{3\alpha}; \quad \rho_\ell = \rho_1 - \frac{4r}{9\alpha}. \quad (8)$$

Such solutions are consistent with our approximations since $[(\rho - \rho_1)/\rho_1] \ll 1$ and $\tilde{D} \Delta \rho \ll v \partial_x \rho$ when $\beta \rightarrow 1$ [42]. In this regime, Eqs. (5)–(8) and simulations of the RMFM yield the same profiles and band velocities. For larger β , the $\tilde{D} \Delta \rho$ term makes fore and rear fronts asymmetric and $c > v$: the flocks fly faster than the birds [42].

Since ρ_ℓ , ρ_h , and m_h do not depend on ρ_0 , increasing the density at fixed temperature only increases the width of the high-density bands. In the thermodynamic limit, phase separated profiles can be seen from ρ_ℓ to ρ_h . One always has $\rho_\ell < \rho_1 < \rho_2 < \rho_h$ so that clusters and homogeneous profiles are linearly stable when $\rho_0 \in [\rho_\ell, \rho_1] \cup [\rho_2, \rho_h]$.

The refined mean-field scenario thus resembles an equilibrium liquid-gas transition in the canonical ensemble, the total magnetization being proportional to the fraction of the liquid phase. Varying the density at fixed temperature, one indeed observes hysteresis loops (see Fig. 2). Increasing ρ_0 , homogeneous disordered profiles are seen up to ρ_1 where the system discontinuously jumps into a phase-separated profile. Further density increases result in a widening of the liquid phase until it almost fills the system for $\rho \lesssim \rho_h$. (The widths of the fronts connecting ρ_ℓ and ρ_h prevent phase-separated profiles for $\rho_0 \approx \rho_{\ell/h}$ in finite systems.) Decreasing ρ_0 , the homogeneous ordered phase remains metastable until $\rho_0 = \rho_2$ before discontinuously jumping to a coexistent state. The fraction of gas then increases until it fills the system at $\rho \approx \rho_l$.

Unlike equilibrium liquid-gas transitions, dense and dilute phases in flocking models have different symmetries. One thus cannot circumvent the transition and continuously transform the system from a gas to a liquid: the transition line cannot stop at a finite point in the (T, ρ_0) plane and, indeed, the critical density is infinite. As far as we are aware, this has not been described for other flocking models [43] even though it should be generic and is consistent with numerical results on the VM [16,27].

Simulations of the 2D active Ising model confirm both the structure of the phase diagram (see Fig. 1) and the nature of the transition predicted by the RMFM. The coexistence between homogeneous and phase-separated profiles is observed and changing ρ_0 at fixed T in the coexistence region only changes the fraction of the liquid phase (see Fig. 2); the velocity of the high density bands, for instance, remains constant [42]. Since high density bands have a minimal size ℓ_c , the apparition of a flock in a finite-size system corresponds to a discontinuous jump to a nonzero magnetization $m_0 \approx m_h \ell_c / L$ which vanishes as

$L \rightarrow \infty$. In this limit, as for a liquid-gas transition in the canonical ensemble, the order parameter varies *continuously* throughout the phase diagram.

The scenario presented here can be related to the measurement of the binder cumulant $G = 1 - (\langle m^4 \rangle / 3 \langle m^2 \rangle^2)$ done in the literature [16,31]. The coexistence between phase-separated profiles ($m = \pm m_0$) and supercooled gas phase ($m = 0$) yields three peaks in $P(m)$ whose weights vary across the transition. (The same holds for the coexistence with superheated liquid.) Assuming a sum of three Gaussians of variance σ , the minimum of G , $G_{\min} = -[12(\sigma/m_0)^2 + 36(\sigma/m_0)^4]^{-1}$, is only markedly negative when $m_0 \gg \sigma$. When $L \rightarrow \infty$, contrary to what happens in a grand-canonical ensemble, both m_0 and σ vanish, the negative peak need not become more pronounced, and the transition may appear critical if σ remains comparable to m_0 (see the 1D case below).

Let us now show that fluctuations strongly alter the transition in 1D. First, all three profiles shown on Fig. 1 exist and are linearly stable in finite systems [44]. The general scenario predicted by the RMFM thus holds: homogeneous profiles are linearly unstable for $\rho_1(T) < \rho_0 < \rho_2(T)$ and phase-separate between linearly stable low-density disordered and high-density ordered regions.

To assess the impact of fluctuations, let us consider the stability of an ordered band in the coexistence region. In 1D, an excess of, say, positive spins on a single site suffices to flip an approaching negative cluster (see Fig. 3); this happens frequently and the total magnetization keeps flipping in this region. The 2D counterpart of such a fluctuation is an excess of positive spins on a transverse band of $\sim L$ sites in front of the approaching cluster, which has a negligible probability when $L \rightarrow \infty$. Similarly, the $m = m_0$ homogeneous profile is unstable in the thermodynamic limit in 1D, which may be why it has not been observed before [44]. Indeed, although a fluctuation leading to a small negative cluster in a uniform profile with $m > 0$ is rare, its probability does not decay exponentially fast with L since only a finite number of sites have to be flipped. When L increases, so does the entropy of such local perturbations; the time it takes to exit the homogeneous state thus vanishes when $L \rightarrow \infty$.

In 1D, only two phases thus survive in the thermodynamic limit: homogeneous disordered profiles and flipping

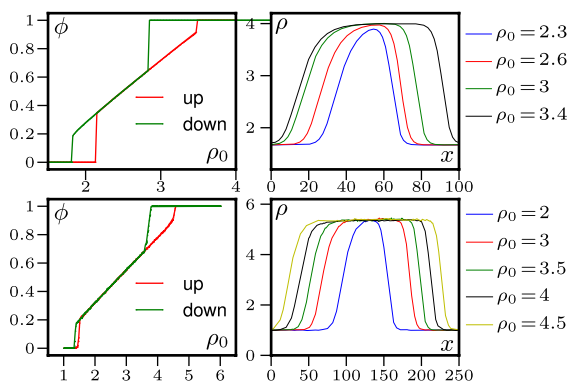


FIG. 2 (color online). Left: Fraction of the ordered liquid phase when ρ_0 is either increased or decreased for the RMFM (top) and in 2D microscopic simulations (bottom). Right: Corresponding profiles of the system. Parameters: RMFM $L = 100$, $v = D = 1$, $r = 1.6$, $\beta = 1.75$, $\Delta\rho_0 = 10^{-2}$ every $\Delta t = 15000$; 2D lattice model $L = 250$, $\beta = 2$, $D = 1$, $\varepsilon = 0.9$, $\Delta\rho_0 = 10^{-2}$ every $\Delta t = 500$.

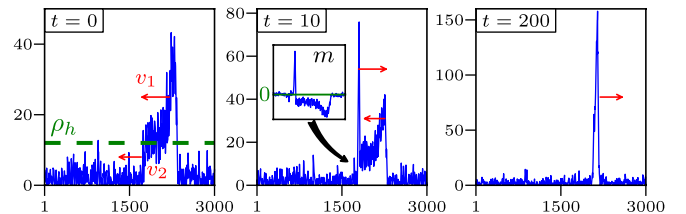


FIG. 3 (color online). Reversal of a 1D cluster due to a localized fluctuation. v_2 is greater than v_1 until $\rho(x) = \rho_h$ in the whole cluster. (See movies in [42].) $\rho_0 = 5$, $D = 1$, $\varepsilon = 0.9$, $\beta = 1.7$.

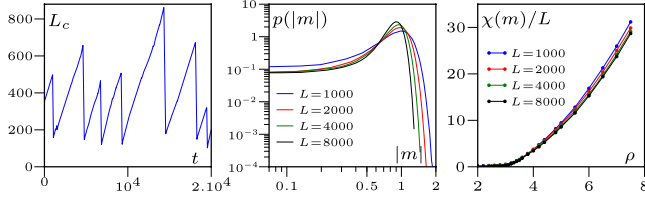


FIG. 4 (color online). Left: Cluster length as a function of time, showing a linear spreading between reversals. $D = 1$, $\varepsilon = 0.9$, $\beta = 2$, $\rho_0 = 3$. Center and Right: $P(|m|)$ for $\rho_0 = 4$; $\chi_m(\rho)/L$; $\beta = 1.538$, $D = 1$, $\varepsilon = 0.9$.

clusters, whose dynamics we now describe (see Fig. 3 and movies in [42]). Starting from a localized cluster, the ordered region spreads at constant speed: the fore front is initially faster than the rear front, their velocity becoming equal when the density in the band has uniformly spread to ρ_h . The mean cluster size before a reversal L_c^R is thus proportional to the mean time between reversals. A reversal corresponds to the progression of a fluctuation from the front to the rear of a cluster, progressively flipping all its sites. The average *duration* of a reversal is thus proportional to L_c^R and hence to the mean time *between* reversals. When $L \rightarrow \infty$, there is a nonzero probability to find the system in a reversal, $P(m)$ does not vanish between $\pm m_0$, and $\langle m \rangle = 0$ (see Fig. 4): there is no spontaneous symmetry breaking in 1D. Since the reversals capture a finite part of the steady-state measure, one cannot replace m by $|m|$ when computing the susceptibility $\chi_m = L(\langle m^2 \rangle - \langle m \rangle^2)$, as is frequently done for the Ising model. In agreement with the lack of ergodicity breaking, and contrary to earlier results in 1D, χ_m is simply extensive in the cluster region.

The difficulty of analyzing Binder cumulants can be clearly seen in 1D, where the large L limit is easily reached and the three peaks in $P(m)$ at the transition can be hard to discriminate. If the width of the peaks is larger than their separation, no negative peak in G is observed. Increasing L does not help since the peaks get closer as they get narrower. In Fig. 5 we show two extreme cases: without the RMFM to analyze the data, it would be very difficult to realize that they correspond to the same transition. This may explain why previous studies of 1D flocking models

with similar—though not identical—dynamics concluded to a second-order transition [22,23].

Conclusion.—We have introduced a lattice model of self-propelled Ising spins whose phenomenology is similar to that of traditional flocking models. The simplicity of our model allows us to show that its flocking transition amounts to a liquid-gas transition in the canonical ensemble with an infinite critical density. The total magnetization is proportional to the liquid fraction and thus varies *continuously* through this first-order transition in the thermodynamic limit, a rather counterintuitive result. This scenario, confirmed numerically in 2D, is altered by fluctuations in 1D, where neither spontaneous symmetry breaking nor critical transitions are observed.

Despite fundamental differences between our model and others found in the literature, such as the symmetry of the order parameter, many features of the flocking transition observed here seem consistent with existing numerical results on either microscopic models [16,19,30] or continuous descriptions [25–28] of self-propelled particles. For instance, the phase diagram seems compatible with those of nematic [19,30] or VM [16,27], even though the high density regions have not been studied in these models. This suggests that the analogy between the flocking transition and a canonical liquid gas transition could be generic, while the symmetry of the order parameter would mostly control features of the ordered phase. For instance, giant-number fluctuations, which have been reported in flocking models, are trivially present in the coexistence region of our model. There, $P(\rho_i)$ is peaked around ρ_ℓ and ρ_h , and the variance of the number of particles in a box of finite size satisfies $\langle N^2 \rangle - \langle N \rangle^2 \propto \langle N \rangle^2$ [45]. They are, however, absent from the homogeneous ordered phase [42], showing that such fluctuations are not intrinsic to polar flocking states.

Active spin models are mostly aimed at improving our theoretical understanding of the flocking transition. One can nevertheless wonder whether such models could be relevant experimentally. The discrete symmetry of the order parameter can for instance stem out of a geometry allowing only two flocking directions, as for locusts in a ring-shaped arena [46,47]. Then, as for the VM, the high density region can only be attained if the interaction range between particles is much larger than their size, as for

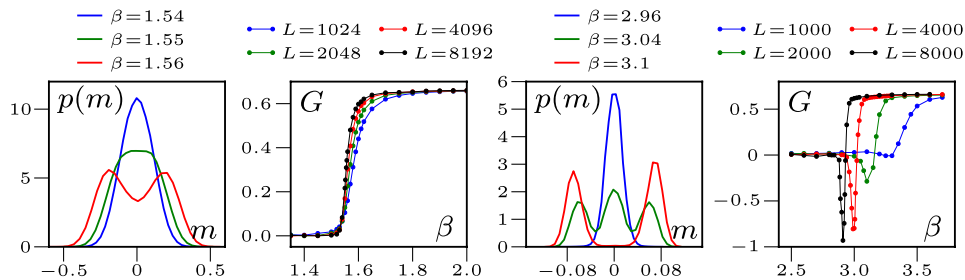


FIG. 5 (color online). Histograms and Binder cumulant of the total magnetization for $\rho_0 = 3$, $D = 1$ (left) and $\rho_0 = 0.2$, $D = 10$ (right). $\varepsilon = 0.9$. $L = 8000$ for $P(m)$.

electrostatic, hydrodynamic, or social interactions. In other cases, such as hard rods, the steric exclusion between particles and other density-induced effects may alter the flocking transition [33]. Lastly, thanks to recent progress on the manipulation of cold atoms in optical lattices, physicists now have a large freedom to control the interactions in spin chains [48]. This could provide an interesting path towards a quantum version of active spin models.

The authors thank H. Chaté, M. Cheneau, G. Grégoire, P. Krapivsky, F. Peruani, H. Touchette, and F. van Wijland for useful discussions.

-
- [1] S. Ramaswamy, *Annu. Rev. Condens. Matter Phys.* **1**, 323 (2010).
- [2] P. Romanczuk, M. Br, W. Ebeling, B. Lindner, and L. Schimansky-Geier, *Eur. Phys. J. Special Topics* **202**, 1 (2012).
- [3] T. Vicsek and A. Zafeiris, *Phys. Rep.* **517**, 71 (2012).
- [4] M. E. Cates, *Rep. Prog. Phys.* **75**, 042601 (2012).
- [5] P. Galajda, J. Keymer, P. Chaikin, and R. Austin, *J. Bacteriol.* **189**, 8704 (2007); P. Galajda, J. Keymer, J. Dalland, S. Parkd, S. Koud, and Rob. Austin, *J. Mod. Opt.* **55**, 3413 (2008).
- [6] J. Tailleur and M. E. Cates, *Europhys. Lett.* **86**, 60002 (2009).
- [7] L. Angelani, R. Di Leonardo, and G. Ruocco, *Phys. Rev. Lett.* **102**, 048104 (2009); R. Di Leonardo, L. Angelani, D. Dell'Arciprete, G. Ruocco, V. Iebba, S. Schippa, M. P. Conte, F. Mecarini, F. De Angelis, and E. Di Fabrizio, *Proc. Natl. Acad. Sci. U.S.A.* **107**, 9541 (2010).
- [8] A. Sokolov, M. M. Apodaca, B. A. Grzybowski, and I. S. Aranson, *Proc. Natl. Acad. Sci. U.S.A.* **107**, 969 (2009).
- [9] J. Schwarz-Linek, C. Valeriani, A. Cacciuto, M. E. Cates, D. Marenduzzo, A. N. Morozov, and W. C. K. Poon, *Proc. Natl. Acad. Sci. U.S.A.* **109**, 4052 (2012).
- [10] I. Theurkauff, C. Cottin-Bizonne, J. Palacci, C. Ybert, and L. Bocquet, *Phys. Rev. Lett.* **108**, 268303 (2012).
- [11] J. Palacci, S. Sacanna, A. P. Steinberg, D. J. Pine, and P. M. Chaikin, *Science* **339**, 936 (2013).
- [12] V. Schaller, C. Weber, C. Semmrich, E. Frey, and A. R. Bausch, *Proc. Natl. Acad. Sci. U.S.A.* **108**, 19183 (2011).
- [13] Y. Sumino, K. H. Nagai, Y. Shitaka, D. Tanaka, K. Yoshikawa, H. Chaté, and K. Oiwa, *Nature (London)* **483**, 448 (2012).
- [14] F. Peruani, J. Starruss, V. Jakovljevic, L. Sogaard-Andersen, and A. Deutsch, M. Bär, *Phys. Rev. Lett.* **108**, 098102 (2012).
- [15] T. Vicsek, A. Czirók, E. Ben-Jacob, I. Cohen, and O. Shochet, *Phys. Rev. Lett.* **75**, 1226 (1995).
- [16] G. Grégoire and H. Chaté, *Phys. Rev. Lett.* **92**, 025702 (2004); H. Chaté, F. Ginelli, G. Grégoire, and F. Raynaud, *Phys. Rev. E* **77**, 046113 (2008).
- [17] F. Peruani, A. Deutsch, and M. Bär, *Phys. Rev. E* **74**, 030904 (2006).
- [18] A. Baskaran and M. C. Marchetti, *Phys. Rev. Lett.* **101**, 268101 (2008); *J. Stat. Mech.* (2010) P04019.
- [19] F. Ginelli, F. Peruani, M. Bär, and H. Chaté, *Phys. Rev. Lett.* **104**, 184502 (2010).
- [20] M. Ballerini, N. Cabibbo, R. Candelier, A. Cavagna, E. Cisbani, I. Giardina, V. Lecomte, A. Orlandi, G. Parisi, A. Procaccini, M. Viale, and V. Zdravkovic, *Proc. Natl. Acad. Sci. U.S.A.* **105**, 1232 (2008).
- [21] F. Ginelli and H. Chaté, *Phys. Rev. Lett.* **105**, 168103 (2010).
- [22] A. Czirók, A.-L. Barabási, and T. Vicsek, *Phys. Rev. Lett.* **82**, 209 (1999).
- [23] O. J. O'Loan and M. R. Evans, *J. Phys. A* **32**, L99 (1999).
- [24] J. Toner and Y. Tu, *Phys. Rev. Lett.* **75**, 4326 (1995); *Phys. Rev. E* **58**, 4828 (1998); J. Toner, *Phys. Rev. Lett.* **108**, 088102 (2012); *Phys. Rev. E* **86**, 031918 (2012).
- [25] S. Mishra, A. Baskaran, and M. C. Marchetti, *Phys. Rev. E* **81**, 061916 (2010).
- [26] A. Gopinath, M. F. Hagan, M. C. Marchetti, and A. Baskaran, *Phys. Rev. E* **85**, 061903 (2012).
- [27] E. Bertin, M. Droz, and G. Grégoire, *Phys. Rev. E* **74**, 022101 (2006); *J. Phys. A* **42**, 445001 (2009).
- [28] T. Ihle, *Phys. Rev. E* **83**, 030901 (2011); arXiv:1304.0149.
- [29] A. Baskaran and M. C. Marchetti, *Phys. Rev. E* **77**, 011920 (2008).
- [30] A. Peshkov, I. S. Aranson, E. Bertin, H. Chaté, and F. Ginelli, *Phys. Rev. Lett.* **109**, 268701 (2012).
- [31] S. Ngo, F. Ginelli, and H. Chaté, *Phys. Rev. E* **86**, 050101(R) (2012).
- [32] Y.-L. Chou, R. Wolfe, and T. Ihle, *Phys. Rev. E* **86**, 021120 (2012).
- [33] F. D. C. Farrell, M. C. Marchetti, D. Marenduzzo, and J. Tailleur, *Phys. Rev. Lett.* **108**, 248101 (2012).
- [34] I. S. Aranson and L. S. Tsimring, *Phys. Rev. E* **71**, 050901 (R) (2005).
- [35] R. A. Blythe and M. R. Evans, *J. Phys. A* **40**, R333 (2007).
- [36] M. R. Evans, Y. Kafri, K. E. P. Sugden, and J. Tailleur, *J. Stat. Mech.* (2011) P06009.
- [37] For $\beta > 3$, should be expanded to higher orders.
- [38] We used spectral methods and fully implicit time stepping to simulate the continuous equations.
- [39] J. Tailleur, J. Kurchan, and V. Lecomte, *J. Phys. A* **41**, 505001 (2008).
- [40] A. G. Thompson, J. Tailleur, M. E. Cates, and R. A. Blythe, *J. Stat. Mech.* (2011) P02029.
- [41] W. Ketterle and N. J. van Druten, *Phys. Rev. A* **54**, 656 (1996).
- [42] See Supplemental Material at <http://link.aps.org/supplemental/10.1103/PhysRevLett.111.078101> for movies and complementary technical details.
- [43] The phenomenological equations of [25,26] focus on the role of propulsion speed and assume finite spinodal densities. Here, we account for the effect of temperature and can thus describe the full phase diagram in the ρ, T plane, hence predicting the $\rho_c = \infty$ critical point.
- [44] Homogeneous ordered phases were not observed in earlier studies of 1D flocking models [22,23]; we numerically checked that they are also present in these models.
- [45] I. S. Aranson, A. Snezhko, J. S. Olafsen, and J. S. Urbach, *Science* **320**, 612 (2008).
- [46] J. Buhl, D. J. T. Sumpter, I. D. Couzin, J. J. Hale, E. Despland, E. R. Miller, and S. J. Simpson, *Science* **312**, 1402 (2006).
- [47] Particles hopping forward correspond to $\varepsilon = 1$.
- [48] T. Fukuhara *et al.*, *Nat. Phys.* **9**, 235 (2013).